Interfaces at the outer boundaries of turbulent motions

By D. K. Bisset, J. C. R. Hunt[1], X. Cai AND M. M. Rogers

1. Motivation and objectives

Most fully developed turbulent flows are inhomogeneous as a result of being blocked by rigid surfaces or by being in contact with regions of very low turbulence or even no motion at all. Inhomogeneity is a pronounced feature of all the canonical shear flows of engineering interest, e.g. wakes, jets, shear layers, and boundary layers. It is observed that the properties of the turbulent motions vary very rapidly at a bounding surface, either approaching a wall or across a highly contorted, moving interface separating the turbulent from the non-turbulent motions.

In relation to the eddy dynamics and statistical properties of the turbulence, the interface

1. delineates the largest scales of the turbulent velocity field L_x;
2. defines the rate of growth of the turbulent velocity field via the mean velocity of the bounding interface normal to itself (E_b);
3. defines, by its convoluted shape, the statistics of intermittency;
4. contains regions of intense local diffusion of vorticity, and of heat and matter; and
5. embodies a vorticity discontinuity where the normal component has to turn itself into a direction parallel to the interface since vortex lines cannot end within the fluid.

The interface is contorted over a range of length scales at least as great as that of the turbulent velocity field, which implies that the local diffusion is very intense (point 4 above); but this does not necessarily imply that the interface becomes diffuse because the eddy motions continuously rebuild the diffusion front. The usual presence of mean velocity E normal to the interface also plays a part. Even when there is no ambient flow, the turbulence generates such mean flows itself through the gradients of the Reynolds stresses provided that it is developing or is non-symmetrical. This motion E induced by the turbulence is also termed an entrainment velocity, but its magnitude and direction are invariably different from those of E_b (Turner 1986).

Components of velocity parallel to the interface might be increased by a vorticity discontinuity (point 5 above), but on the other hand they might decrease because they have no contribution from induction by the vortex lines that would have been

1 Permanent address: Cambridge University, DAMTP, Silver Street, Cambridge, UK

there in the absence of the interface (Carruthers & Hunt 1986). The fact that the vorticity is parallel while there is some component of fluctuating velocity normal to the interface suggests that the local helicity ($h \equiv \vec{\omega} \cdot \vec{u}$) is small; in fact, normalized h may become smaller as E_b becomes greater (Hunt & Hussain 1991).

Knowing more about the kinematic features of these interfaces will be useful for examining the implications of concepts and models that make simplifying assumptions about their large- and small-scale shape [which range from being flat (Phillips 1955) to fractal (Sreenivasan & Meneveau 1986)] and about their intermittency (Townsend 1976). The dynamics will be better understood when the rapid changes in the vorticity and velocity components are measured and studied in local frames to see if they are locally determined or whether they are essentially determined by the largest scales of the flow (Gartshore 1966). Additionally, the movement of fluid particles relative to the interface is the essential quantity to simulate, measure, and analyze in order to calculate how the interface affects the mixing of scalar quantities and thence how it controls chemical reactions and combustion. The *turbulent* interface considered here is not the viscous superlayer (Corrsin & Kistler 1955) that has a thickness of the order of the Kolmogorov lengthscale, though the superlayer could fall within it.

Some of the specific questions we are examining are the following.

1. What determines the interface propagation velocity E_b? In other words, for an unbounded turbulent shear flow, how does non-turbulent fluid become turbulent? We know that, in the limit, it happens through molecular diffusion across local regions of large velocity gradient and that such regions occur because of:
   - engulfment of irrotational fluid, which is then mixed deep within the flow, and
   - straining (stretching) motions in the vicinity of the turbulent/non-turbulent interface.
   - Are there other possibilities?

   Consider also detrainment, where isolated regions of rotational fluid detach and drift outwards. (See also the studies of Hunt, Durbin & Wu in this volume.)
2. What are the essential features of the interface (whether defined in terms of velocity, vorticity, and combinations such as helicity or scalar quantities and/or their derivatives) and are they distinct enough to define the interface?
3. (a) How can such an interface be defined unambiguously, especially since it may be multiply connected? (b) How can its 3D position and orientation (outward normal) be determined as $f(x, y, z, t)$ in the DNS data? [The answer depends on how distinct it is.]
4. What are the values of various properties in the vicinity of the interface (vector and scalar variances, correlations, ...)?
   - Are there systematic variations, e.g. differences between the outer face and inner face of a protrusion?
   - Are there any interesting changes in properties over time or changes in the interface shape (e.g. during engulfment)?

5. What are the characteristics of irrotational fluid that has moved away from its free-stream state? [Such fluid may contribute to mass flux, for example.]
6. Is there a dependence on Reynolds number, spreading rate, flow type, the nature of the DNS simulation, or other parameters (for example forcing, which clearly increases intermittency and the depth of the convolutions) for any of the above?

2. Accomplishments

The project is still in its early stages, and only a few of the above questions have been addressed so far. All of the work mentioned here utilizes the simulations of a temporally growing, self-preserving turbulent far-wake reported by Moser, Rogers & Ewing (1998). The data set stored at $\tau = 43$ was used for scalar detection work, and the data from $\tau = 91$ were used for vorticity-based detection.

2.1 Interface detection through scalar level

A preliminary investigation of interface properties was carried out by X. Cai using the level of a passive scalar as the interface detection criterion. Under some conditions the scalar can mark vortical regions quite accurately, and unlike vorticity, the scalar has exact, constant bounds to its range of values. Two main advantages result from this. First, detection threshold levels are likely to remain constant over time, and second, the level of numerical noise relative to thresholds can be assessed through examination of out-of-range values of the scalar. However, the way in which the scalar was initialized within the present DNS was aimed at a study of the transfer of fluid from one side of the wake to the other, and therefore the correspondence between scalar-marked regions and vortical regions is not always close, even at later times. The scalar was initialized with value 0.0 in the free-stream *below* the starting field of the turbulent wake and at 1.0 *above* it, with a smooth gradation of values within the turbulence. Nevertheless, these initial results suggest that the interface is very sharp, but that results may depend on the details of the detection procedure and threshold values used. A summary of this work is attached as an appendix.

2.2 Interface detection through vorticity

For current work we are using ω, the magnitude of the vorticity vector, for detection of the turbulent/non-turbulent interface, which should be more reliable than the passive scalar for the present DNS data. At very low levels, however, ω is affected by numerical noise. The magnitude of the noise problem depends on the intrinsic sharpness of the interface; if the interface is sharp, its detection should be relatively independent of the level of ω over some range, and a level slightly above any background noise can be used. Noise particularly affects the calculation of the direction of the normal to the interface.

Conditional averaging outside and inside the interface should be carried out along a line normal to the interface, which involves careful interpolation of data. Stored data in spectral form were projected onto a relatively fine, uniform physical grid of $385 \times 400 \times 97$ points so that linear interpolation between gridpoints would be accurate. For simplicity, the present results are confined to a subset of the data for

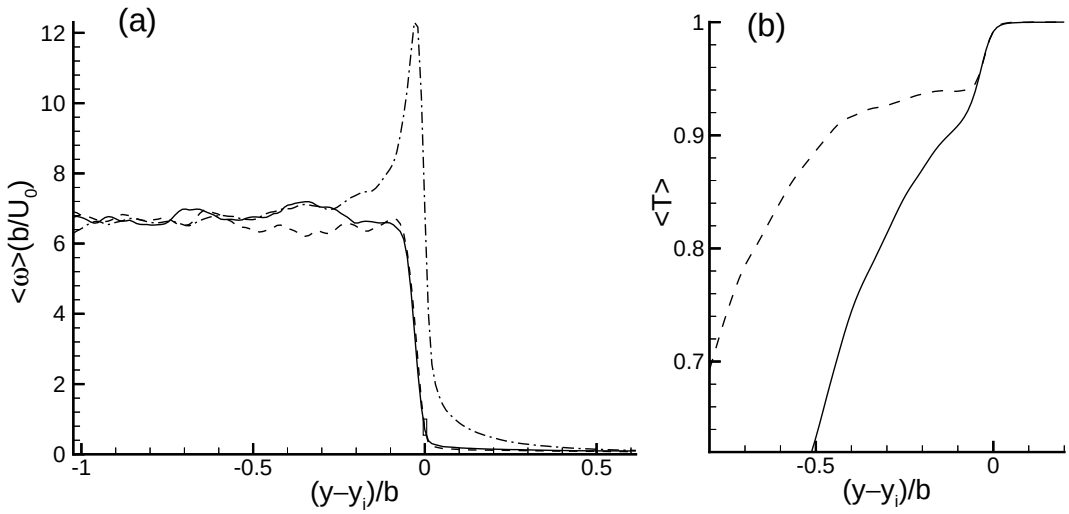

FIGURE 1. Effects of detection parameters on (a) vorticity magnitude, and (b) level of passive scalar, relative to the turbulent/non-turbulent interface. ——— inner group for $C_\omega = 0.7U_0/b$; - - - - outer group for $C_\omega = 0.7U_0/b$; —·— $C_\omega = 7U_0/b$

which the surface normal is within 25^o of the y-axis (normal to the wake centerplane), and conditional averaging is carried out in the y-direction only (with linear interpolation). Both sides of the wake are used, with sign reversal as appropriate. Only the outermost crossing of the vorticity threshold for any (x, z) position is considered in each case. Further interface positions resulting from irrotational fluid intruding below the detected vortical fluid (which certainly happens here and there) are ignored.

The lowest level of the detection threshold C_ω that seemed to give reliable interface detections was $0.7U_0/b$ (U_0 is the centerline velocity defect and b the wake width across the half-mean-velocity points); this level is used below unless stated otherwise. The interface indeed appears to be quite sharp in that substantial increases in C_ω had only small effects on detected positions, and conditional averages show little vorticity outside the interface. After application of the 25^o angle criterion, about 26% of the surface area projected onto the centerplane was accepted.

The direction of the normal may in itself be significant for the properties of the interface, as may be its position on a protrusion or at the depths of an irrotational intrusion, and therefore other criteria may be used in conjunction with ω level. In particular, the main set of interface positions was split into three equal-size subsets according to whether the interface was roughly its average distance from the centerplane, or significantly closer, or further away (the last two being the 'inner' and 'outer' subsets for the following results).

The effects of threshold level and the inner/outer split on $\langle\omega\rangle$ are shown in Fig 1a. Angle brackets indicate conditional averaging relative to the detected interface at y_i while an overbar indicates a conventional average. For the main set of detections,

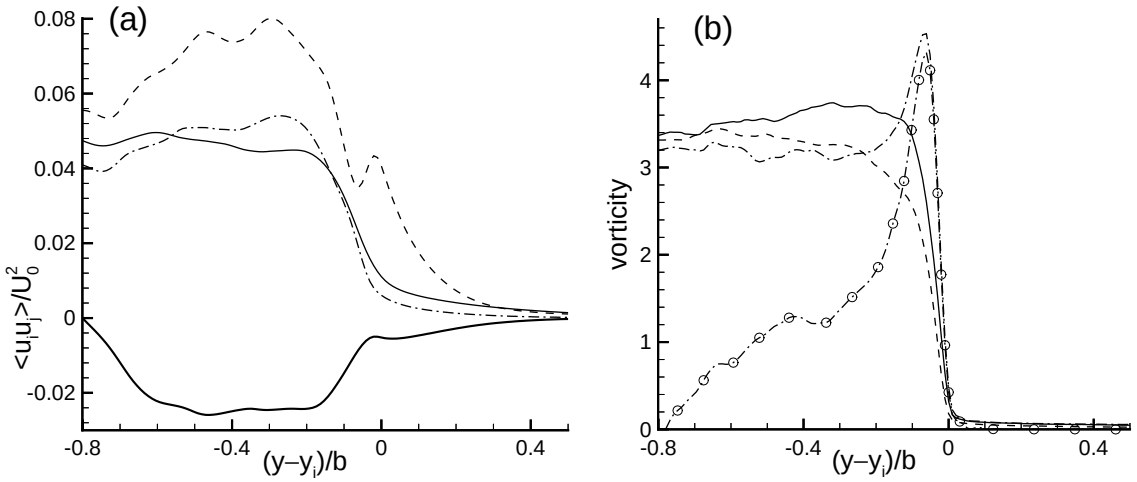

FIGURE 2. Normalized Reynolds stresses and vorticity components for $C_\omega = 0.7U_0/b$. (a) – – – – $\langle u^2\rangle$; ——— $\langle v^2\rangle$; —·— $\langle w^2\rangle$; lowest curve is $\langle uv\rangle$. (b) ——— $\langle|\omega_x|\rangle$; – – – – $\langle|\omega_y|\rangle$; —·— $\langle|\Omega_z|\rangle$; · · · ○ · · · $-\langle\Omega_z\rangle$.

the distribution of $\langle\omega\rangle$ (not shown) is very similar to the inner and outer curves. Increasing C_ω by a factor of ten results in the appearance of a thin layer of very high $\langle\omega\rangle$, but there is a significant 'leakage' of vorticity into the irrotational region (Fig 1a). Also there is a reduction in the number of accepted points from 26% to 17% of the projected surface area here, leaving only the strongest regions for averaging. It turns out that there is very little difference for $\langle\omega\rangle$ between the inner and outer subsets (other quantities behave differently, as will be demonstrated).

The turbulent zone of the wake has almost uniform vorticity (Fig 1a), and the gradient at the interface is quite sharp. This gradient is not an artifact of the detection process: the tiny rectangle near $y = y_i$ shows a typical separation between adjacent data levels/gridpoints that confine the detected interface, and the threshold-based detection merely requires that the $\langle\omega\rangle$ curve should pass down through that rectangle.

Corresponding to the region of high gradient in $\langle\omega\rangle$, there is a large gradient of the scalar $\langle T\rangle$ (Fig 1b) that is almost identical for the inner and outer subsets. In terms of conditional averages, agreement between the interface and the edge of the scalar-marked zones seems remarkably good given the reservations expressed earlier, but it could be worse for surfaces not roughly parallel to the centerplane. Within turbulent zones there is a divergence between the inner and outer subsets, presumably related to the greater distance from the source of 'cold' scalar in this case, but it is not clear why there should then be such similarity within the interface.

Reynolds stresses relative to the interface and a breakdown of the components of ω are shown in Fig. 2 (all subsets combined). As expected, Reynolds stress levels for the interior of the wake are much the same as for the conventionally averaged case (Moser, Rogers & Ewing 1998) with some flattening of the peaks in $\overline{w^2}$ and

$\overline{uv}$. The levels of fluctuations induced in the irrotational zone are not negligible and decrease only slowly outside the interface — these are potential fluctuations, not 'leakage'. Gradients within turbulent zones near the interface (i.e. the slopes of the curves shown) are not as steep as for $\langle\omega\rangle$, which is presumably because of the greater contribution from large-scale structures to Reynolds stresses than to vorticity. It is conceivable that large increases in Reynolds number would steepen these gradients and eventually cause local maxima in $\langle u^2\rangle$ and $\langle w^2\rangle$, as suggested by Carruthers & Hunt (1986). The moderate-sized peak in $\langle u^2\rangle$ presently existing just inside the interface, which continues into the irrotational zone, is a result of the conventional (i.e. Reynolds averaging) definition of u^2 as $(U - \overline{U}(y))^2$, to be discussed shortly. Results for the inner and outer subsets taken separately (not shown) differ a little quantitatively but not qualitatively.

By symmetry $\langle\omega_x\rangle$ and $\langle\omega_y\rangle$ should be zero for surfaces parallel to the centerplane, so their magnitudes $\langle|\omega_x|\rangle$ and $\langle|\omega_y|\rangle$ are presented along with $-\langle\Omega_z\rangle$ and $\langle|\Omega_z|\rangle$ in Fig. 2b (Ω_z includes the non-zero mean spanwise vorticity). As noted earlier, the normal component ω_y is expected to decrease first as the interface is approached, which is verified by the results, while the parallel components exhibit sharper cutoffs. The peak in $-\langle\Omega_z\rangle$ is a result of the direct contribution from mean shear $d\overline{U}/dy$ for surfaces in the present orientation, and it appears that almost all ω_z has the same sign close to the interface. Spanwise vorticity $\langle\Omega_z\rangle$ changes sign across the midplane while its magnitude $\langle|\Omega_z|\rangle$ is nearly constant and similar to the other two magnitudes. Results for surfaces in other orientations may turn out differently.

The conventional mean velocity $\overline{U}(y)$ is compared to $\langle U\rangle$ in Fig. 3a, with the latter curve offset along the x-axis by the average height of interface detections. The gradient in $\langle U\rangle$ is quite sharp, and it is clear that the gentle rolloff in $\overline{U}$ is a result of a statistical distribution of superimposed instantaneously sharp dU/dy events. The larger difference between the two curves in the vicinity of the interface is the explanation for the extra peak in $\langle u^2\rangle$ seen in Fig. 2a, given the conventional definition of fluctuation u.

Conditional mean velocities for the inner and outer subsets show considerable differences (Fig. 3b). Both groups show a large gradient and sharp cutoff in $\langle U\rangle$, but just outside the interface the level of $\langle U\rangle$ is quite different: it is well below its free-stream value for the inner subset and significantly above free-stream for the outer subset. Presumably these are potential-flow effects caused by large protrusions of turbulent fluid either blocking or 'squeezing' the free-stream flow. Transverse velocity $\langle V\rangle$ for the outer group is dominated by a strong outwards flow ($\langle V\rangle$ reaches more than 12% of U_0) in the region inside the interface, suggesting quite active growth of the outer regions of the interface. The dominant feature for the inner group is an inwards flow in the region outside the interface; it is tempting to call this an entrainment flow although we don't know how the interface is moving relative to the fluid at this stage.

2.3 Tentative conclusions

The picture emerging so far, largely in agreement with the concepts of Townsend

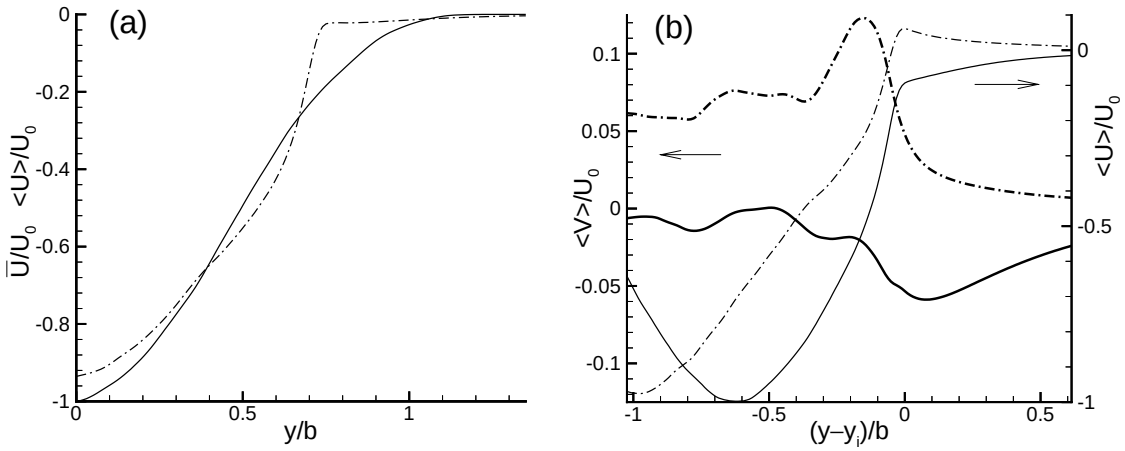

FIGURE 3. Mean velocity distributions. (a) ——— $\overline{U}$; —·— $\langle U \rangle$ offset by $y = 0.75b$ (all detections). (b) ——— inner subset; —·— outer subset.

(1976) and others, is that the far-wake consists of relatively uniform zones of well-developed turbulence bounded by a convoluted, rather sharp interface. Gradients of velocities, vorticity, and passive scalar are very steep through the interface until they suddenly flatten out at the free-stream. Both velocity fluctuations and systematic deviations in mean velocities $\langle U \rangle$ and $\langle V \rangle$ are quite significant within the irrotational regions near the interface. It will be very important to investigate and describe quantitatively the shape and movement of the interface, which is likely to be a function of the large-scale organized motion of turbulent flow. Additionally, there is at least the possibility of differences at much higher Reynolds numbers than that of the present simulation.

3. Future plans

Because this project is at an early stage, the quickest summary of future plans is to say that we will continue to study the six questions posed in Section 1. To begin with, we will extend the current procedures to regions where the interface is *not* roughly parallel to the wake centerplane.

In addition to the above, we plan to

- examine locally interesting regions including topological features both on and just inside the interface
- develop a means of describing concisely the shape of the interface
- use the unique time-dependent DNS results to determine how the interface moves and changes shape and to determine where and how it moves into irrotational fluid.

Data from the wake simulations with large-scale forcing (Moser, Rogers & Ewing 1998), which show a large increase in the sizes and heights of protrusions and intrusions, may be very useful for these purposes.

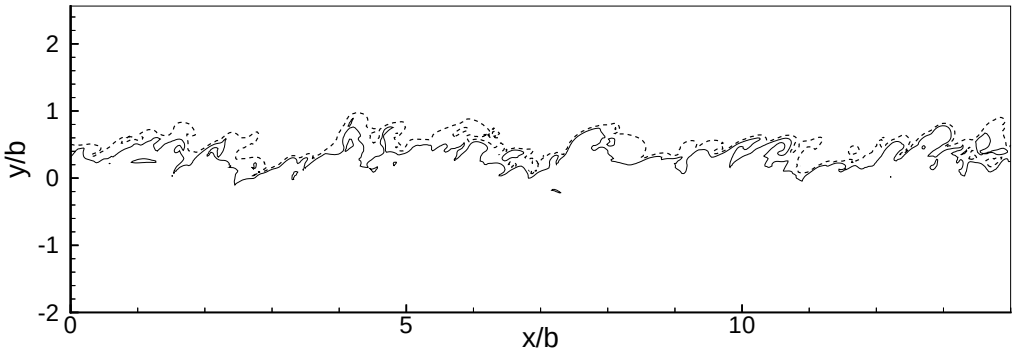

FIGURE A1. Typical interfaces at $C_s = 0.90$ (———) and $C_s = 0.99$ (----).

Appendix: Passive scalar detection of turbulent/non-turbulent interfaces

by Xiaodan Cai

A passive scalar has been used to outline the boundary of turbulent and non-turbulent flow in experimental works, e.g. Weir, Wood and Bradshaw (1981). A traditional reason for this is that the passive scalar obeys the same advective-diffusive equations as the vorticity for two-dimensional flow (given a Prandtl/Schmidt number of order 1). In some flows, such as wakes and mixing layers, the interface between turbulent and non-turbulent flow is dominated by two-dimensional vortical structure. Hence, it is expected that the passive scalar can give a good description of the interface. Based on such observations, an interface-detector is developed in this study. The algorithm for it is to search through the whole scalar field, which is constructed by a linear-interpolation from the calculated discrete values, for the surface with a specific scalar concentration (C_s). This technique is applied to a DNS database of a three-dimensional time-evolving plane wake (Moser, Rogers & Ewing 1998). The wake has reached an approximately self-similar state with a mass-flux Reynolds number (equal to the momentum thickness Reynolds number in spatially developing wakes) of 2000, which is high enough for a short $k^{-5/3}$ range to be evident in the streamwise one-dimensional velocity spectra. A passive scalar is advected within the wake and has a value of one (or zero) in the upper (or lower) external nonturbulent region. Here only the upper interface is analyzed. Fig. A1 shows the scalar contours for typical configurations of the interfaces at the threshold levels of 0.90 and 0.99. The interfaces are almost continuous, and there exist only very few islets.

Five threshold values have been tried for the passive scalar to define the upper interface in this study. Fig. A2 shows the probability density functions for the interface locations. All of the pdf's are approximately Gaussian with a skewness around zero and a flatness around 3.0, as shown in the Table. It is noted that the mean locations of the interface increase with the threshold values and that the interface can even cross the centerline to the lower part of the wake when $C_s \leq 0.9$.

Based on these observations, two sampling methods were investigated to calculate

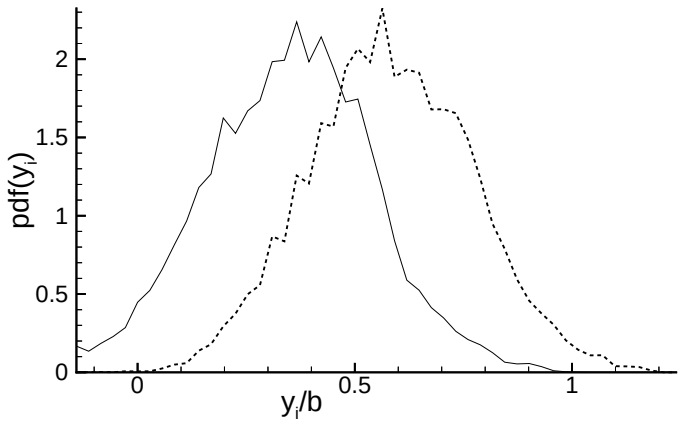

FIGURE A2. Probability density functions of interface positions for thresholds 0.9 (———) and 0.99 (- - - -).

TABLE. Statistics of the interface positions

C_s	$\overline{y_i}/b$	y_i'/b	S_i	F_i
0.85	0.27	0.18	0.34	3.05
0.90	0.36	0.19	− 0.016	2.96
0.95	0.46	0.19	0.025	2.93
0.98	0.55	0.19	0.072	2.89
0.99	0.59	0.21	− 0.69	2.92

the conditional ensemble averages along y relative to the interface. Method I is to select the lowest y points as the locations of the interface whenever islets or multi-folded regions appear. Method II is to leave off the regions from the sampling space whenever islets or multi-folded regions appear. The sampling space is limited to the upper half of the wake. In order to increase the sampling points and reduce the statistical errors, a bar with 0.2 length-unit (based on the momentum thickness) wide is used to collect the samples and labeled according to the distance of its center from the interface. The conditional velocity intensities from the two sampling methods displayed very similar characteristics; Method II is used for the following results. Distributions of u^2, v^2, and w^2 (longitudinal, transverse, and spanwise components respectively) relative to the interface are shown in Fig. A3. Inside the turbulent region, $\langle v^2 \rangle$ is relatively uniform while $\langle u^2 \rangle$ and $\langle w^2 \rangle$ increase to a peak value when approaching the interface, which is consistent with the linear theory prediction by Carruthers and Hunt (1986). In the non-turbulent region, it can be seen that all of the velocity intensities decay towards zero sufficiently far from the interface, and there exists a region where $\langle u^2 \rangle \approx \langle v^2 \rangle + \langle w^2 \rangle$ and $\langle v^2 \rangle \approx \langle w^2 \rangle$, as predicted by the Phillips (1955) theory on the irrotational motion induced by the turbulent boundary flow. These phenomena prevail even when the threshold values are changed (Fig. A3).

Fig. A4 presents the distributions, for different threshold values, of conditional

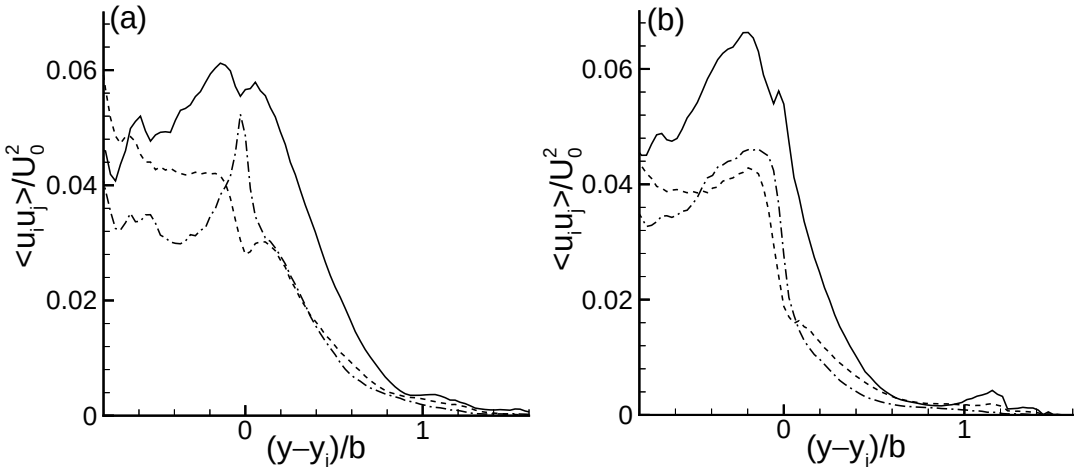

FIGURE A3. Distributions of —— $\langle u^2 \rangle$, - - - - $\langle v^2 \rangle$ and —·— $\langle w^2 \rangle$ relative to the interface for threshold values (a) 0.90 and (b) 0.99

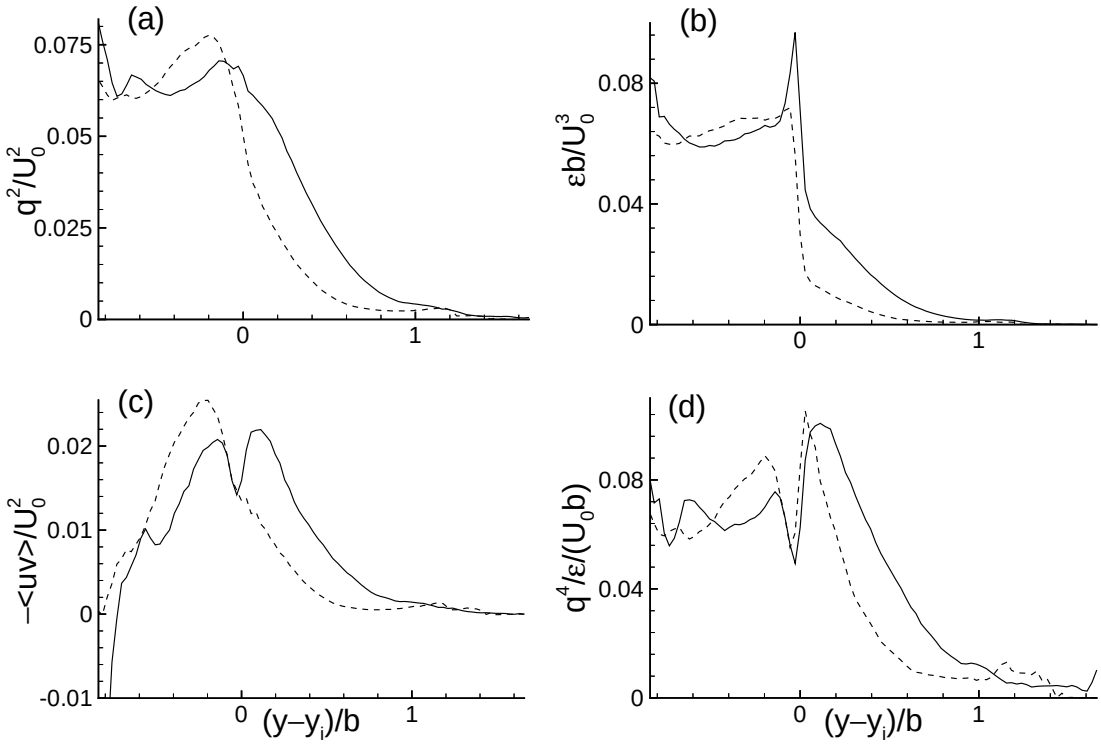

FIGURE A4. Distributions of various conditionally-averaged quantities for threshold values 0.9 (——) and 0.99 (- - - -): a) q^2; b) ε; c) $-\langle uv \rangle$ and d) q^4/ε.

averages of turbulent energy q^2, dissipation rate ε, turbulent shear stress $-\langle uv \rangle$, and turbulent viscosity q^4/ε. Vorticity, and hence dissipation rate, should drop sharply across the turbulent/nonturbulent interface, which is demonstrated in Fig. A4(b). Furthermore, it is noted that the larger the threshold values, the sharper the edge between the turbulent and nonturbulent region, which is a good indication that the above-proposed interface detector works well in this wake flow. It also can be seen that the larger the threshold values, the more physical the results appear to be. As the threshold value increases, the peaks around the interface in Fig. A4(b) are weakened and finally disappear, and the peaks of turbulent shear stress in Fig. A4(c) shift from the nonturbulent side to the turbulent side. Physically, it can be argued that the turbulent shear stress cannot be generated by mean shear rate in irrotational flow, and therefore the peak values in the nonturbulent flow are unphysical. Meanwhile, it can be argued that there may exist different fluctuating kinetic energy-generation mechanisms inside and outside the interface. Inside the interface, the velocity fluctuations are generated by the mean shear rate, which results in a quite uniform value for q^4/ε in Fig. A4(d), while outside the interface, the velocity fluctuations are generated by the turbulent interface, which is the topic studied by Phillips (1955). This argument may explain why there is a big dip around the turbulent/nonturbulent interface in Fig. A4(d).

REFERENCES

Carruthers, D. J. & Hunt, J. C. R. 1986 Velocity fluctuations near an interface between a turbulent region and a stably stratified layer. *J. Fluid Mech.* **165,** 475-501.

Corrsin, S. & Kistler, A. L. 1954 *NACA Tech Note 3133.*

Gartshore, I. S. 1966 An experimental examination of the large-eddy equilibrium hypothesis. *J. Fluid Mech.* **24,** 89-98.

Hunt, J. C. R. & Hussain, F. 1991 A note on velocity, vorticity and helicity of inviscid fluid elements. *J. Fluid Mech.* **229,** 569-587

Moser, R. D., Rogers, M. M. & Ewing, D. W. 1998 Self-similarity of time-evolving plane wakes. *J. Fluid Mech.* **367,** 255-289.

Phillips, O. M. 1955 The irrotational motion outside a free boundary layer. *Proc. Camb. Phil. Soc.* **51,** 220.

Sreenivasan, K. R. & Meneveau, C. 1986 The fractal facets of turbulence. *J. Fluid Mech.* **173,** 357-386.

Townsend, A. A. 1976 *The Structure of Turbulent Shear Flow,* 2nd ed. Cambridge University Press.

Turner, J. S. 1986 Turbulent entrainment: the development of the entrainment assumption and its application to geophysical flows. *J. Fluid Mech.* **173,** 431-471

Weir, A. D., Wood, D. H. & Bradshaw, P. 1981 Interacting turbulent shear layers in a plane jet. *J. Fluid Mech.* **107,** 237.